Chinese Chemical Letters 32 (2021) 3483–3486

Contents lists available at ScienceDirect

Chinese Chemical Letters

journal homepage: www.elsevier.com/locate/cclet

Communication

−22-Fold of ^{1}H signal enhancement *in-situ* low-field liquid NMR using nanodiamond as polarizer of overhauser dynamic nuclear polarization

Zhen Zhang[a,b], Fang Chen[a,b,*], Jiwen Feng[a,b], Junfei Chen[a,b], Li Chen[a,b], Zhi Zhang[a,b], Huijuan Wang[a,b], Xin Cheng[a,b], Maili Liu[a,b,c], Chaoyang Liu[a,b,c,*]

[a] State Key Laboratory of Magnetic Resonance and Atomic and Molecular Physics, Wuhan Center for Magnetic Resonance, Wuhan Institute of Physics and Mathematics, Innovation Academy for Precision Measurement Science and Technology, Chinese Academy of Sciences, Wuhan 430071, China
[b] University of Chinese Academy of Sciences, Beijing 100049, China
[c] Wuhan National Laboratory for Optoelectronics, Huazhong University of Science and Technology, Wuhan 430074, China

ARTICLE INFO

Article history:
Received 3 February 2021
Revised 17 March 2021
Accepted 28 May 2021
Available online 31 May 2021

Keywords:
ODNP
Polarizer
Nanoparticle
Enhancement
Relaxation

ABSTRACT

Nanodiamond (ND) polarizer can be used for dynamic nuclear polarization (DNP), owing to unpaired electrons provided by surface defects. However, ^{1}H enhancement *via* Overhauser DNP (ODNP) using ND *in-situ* liquid has been found much smaller than traditional radicals. Herein, we study the surface properties of ND using electron spin resonance (ESR) and Raman methods firstly. Then the enhancement of ^{1}H ODNP is explored using ND as polarizer with different nanoparticle sizes and concentrations at home-built 0.06 T DNP spectrometer. The surface of ND with the size of 30 nm is further modification *via* high temperature air oxidized and the enhancement was measured. The results show that nanoparticle sizes and Raman peak intensity ratio of sp^2/sp^3 hybridization are approximate negative correlation and positive correlation to enhancement, respectively. Furthermore, there is no significant enhancement in the oxidation group, and a −22.5-fold ^{1}H ODNP enhancement is achieved *in-situ* liquid at room temperature, which demonstrate the ND can be used as an efficient enhancer. We expect ND to play a greater role in biomedical research, especially for multimodal imaging with improving the performance of ND surface.

Nanodiamond (ND) has a promising application in drug delivery and fluorescence imaging, benefiting from its advantages of chemical stability and surface modifiability [1–3]. Moreover, ND can be used for Magnetic Resonance Imaging (MRI) as contrast agent owing to surface defects. More importantly, because of these excellent characteristics, ND provides the possibility of bimodal biological images (*e.g.*, fluorescence image and MRI), thus offering more information of tissue structure [4]. However, as an application of nuclear magnetic resonance (NMR), the signal-to-noise ratio of MRI is proportional to polarization of nucleus spins in thermal equilibrium and is thus very low compared with highly sensitive fluorescence method. How to improve the polarization of nuclear spins even to achieve nuclear hyperpolarization has become a hot topic of NMR [5,6]. Overhauser dynamic nuclear polarization (ODNP) is one of the widely used polarization methods [7]. ODNP technique transfers larger polarization of electrons to nuclei *via* electron-nucleus interactions, so as to greatly increase the polarization of ^{1}H [8]. Theoretically, ^{1}H polarization could be enhanced about 660 times due to gyromagnetic ratio of electron (γ_S) is approximately 660 times of proton (γ_I). ODNP requires the participation of unpaired electrons from radicals. The commonly used organic radicals are toxic to organisms, which is not conducive to biomedical research. It is highly urgent to find potential biological safety radicals. This dilemma may be solved by ND [9]. Especially for study of biological models, the application of DNP in low-field has broader prospects, since its advantages of weak microwave heating effect, larger skin depth, larger sample space and in situ experiment compared with high-field DNP [10–12].

ND polarizer dispersed in liquid used for ^{1}H enhancement *via* ODNP has been reported. Waddington *et al.* achieved ^{1}H NMR enhancement to −4-fold at 6.5 mT [13]. However, the yielded enhancement of ^{1}H by ND polarizer is much lower than traditional organic radicals which can achieve hundreds of times enhancement [14]. As far as we know, ^{1}H NMR enhancement *via* ND in low-field liquid DNP is still very small and cannot fully meet the demand for research. In order to realize the application of ND as

* Corresponding authors at: State Key Laboratory of Magnetic Resonance and Atomic and Molecular Physics, Wuhan Center for Magnetic Resonance, Wuhan Institute of Physics and Mathematics, Innovation Academy for Precision Measurement Science and Technology, Chinese Academy of Sciences, Wuhan 430071, China.
E-mail addresses: chenfang@wipm.ac.cn (F. Chen), chyliu@wipm.ac.cn (C. Liu).

https://doi.org/10.1016/j.cclet.2021.05.068
1001-8417/

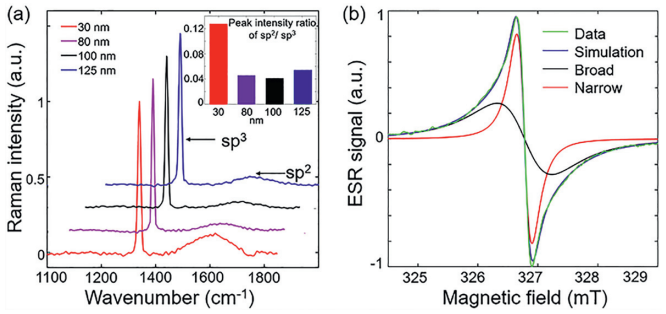

Fig. 1. (a) Raman spectra of four sizes ND and illustration is peak intensity ratios of sp^2/sp^3; (b) ESR spectra of 30 nm ND.

DNP polarizer, it is of great necessity to largely improve the performance of ND polarizer.

Surface properties of ND and enhancement are tightly bound. Herein, we investigate a series of different nanoparticle size of NDs which may contain more unpaired electrons on surface. Electron spin resonance (ESR) and Raman spectroscopy are employed to investigate paramagnetic defects and carbon dangling bonds on ND surface, so as to evaluate the potential of ND used in ODNP. Then, ODNP experiments of ^{1}H NMR enhancements (Section 1 in Supporting information) in ND-dispersed water are carried out on homemade 0.06 T DNP spectrometer [14]. The influence of nanoparticle sizes and concentrations of ND on ^{1}H enhancement is explored. Finally, the factors affecting enhancement of actual ND sample are discussed to further improve the performance of ND polarizer *via* the experiments of 30 nm air oxidized ND.

According to Raman spectra of NDs including four sizes in Fig. 1a, two types of carbon atoms are found. The sp^3 and sp^2 hybridization come from the carbon phase in core of ND at wavenumber of 1332 cm^{-1} and on ND surface at wavenumber of 1580 cm^{-1}, respectively [15]. The sp^2 carbon provides not only unpaired electrons, but also adsorption sites for water molecules. For spherical nanoparticle materials, the larger specific surface area (SSA) arises from the smaller nanoparticle size (r) (SSA = $3/r$). According to illustration of Fig. 1a, Raman peak intensity ratios of sp^2/sp^3 with 30 nm ND is nearly 3-fold higher than large-size NDs, which is coincident with SSA, indicating that sp^2/sp^3 is positive correlation with SSA: SSA$\sim \delta(sp^2/sp^3)$, where $\delta(sp^2/sp^3)$ represents the weight of sp^2 carbon. The 30 nm ND may contain more unpaired electrons on surface than large-size NDs. We further analyzed ESR of 30 nm ND at 0.1 mg/μL, as shown in Fig. 1b. ESR spectra comprised two components by fitting. The narrow component is assigned to defects located in ND core, and broad component is from carbon dangling bonds on ND surface [16]. The proportion of broad component area in ESR spectrum is about 90%, and concentration is approximately 10^{19} spin/g [17]. From these results, NDs used in our experiments may be suitable as ODNP polarizer.

The schematic of ODNP process is exhibited in Fig. 2a. The ^{1}H NMR enhancement of ODNP with four nanoparticle sizes of ND at 0.06 T with 0.1 mg/μL are shown in Fig. 2b. With the increase of microwave (MW) power, ^{1}H NMR enhancement increases and finally tends to saturation. ^{1}H enhancement (E_{exp}) with 30 nm is higher than large-size NDs, which is consistent with the larger Raman peak intensity ratio of sp^2/sp^3 (Table 1). Consequently, Raman spectra provides a good assistant method to evaluate the potential of ND for ODNP by crudely classifying ND based on sp^2/sp^3, ($E_{exp} \sim \delta(sp^2/sp^3)$).

In order to explore the maximum enhancement of ^{1}H NMR, a series of experiments with 30 nm were implemented at different concentrations as shown in Fig. 2c and we achieved experimental maximum values (E_{exp}) of −22.5-fold at 0.5 mg/μL in Fig. 2d.

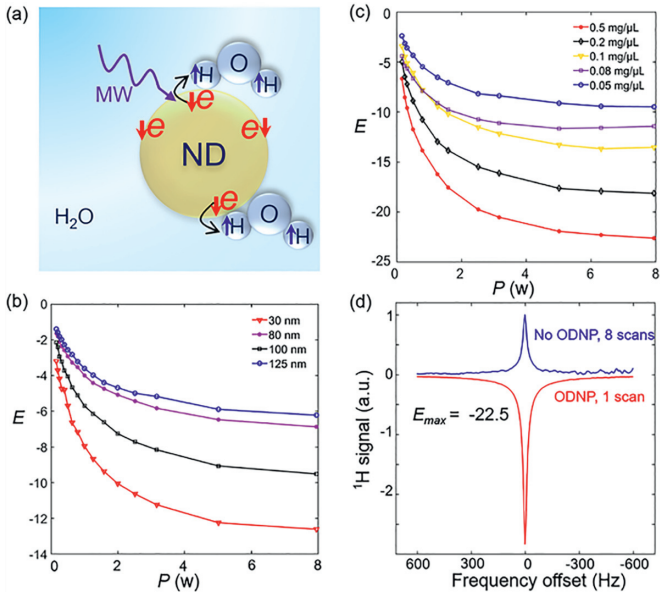

Fig. 2. (a) The transfer of polarization from unpaired electron on ND surface to ^{1}H with MW irradiation; (b) ^{1}H NMR enhancements in four nanoparticle sizes ND solution at 0.1 mg/μL *vs.* MW power; (c) ^{1}H NMR enhancements in five concentrations of 30 nm ND solution vs. MW power; (d) ^{1}H NMR spectra with and without ODNP at 0.06 T.

Table 1
Raman peak intensity ratio of sp^2/sp^3, T_1, T_2, and E_{exp} of ^{1}H in four sizes ND solution at 0.1 mg/μL at 0.06 T.

ND (nm)	sp^2/sp^3	T_1 (ms)	T_2 (ms)	E_{exp}
30	0.125	410	209	−13.7
80	0.044	478	312	−7.17
100	0.039	403	266	−10.7
125	0.054	450	315	−6.1

Table 2
Parameters of ^{1}H enhancement in five concentrations of 30 nm ND solution at 0.06 T.

C (mg/μL)	T_1 (ms)	T_2 (ms)	E_{exp}	E_{max}
0.5	150	43	−22.5	−24.2
0.2	240	82	−18.1	−19.5
0.1	410	209	−13.7	−14.9
0.08	635	260	−11	−12.4
0.05	750	373	−8.9	−10.3

To the best of our knowledge, this is the greatest 1H signal enhancement in liquid using ND polarizer in-situ low field DNP. The approximate experimental (E_{exp}) and theoretical maximum values (E_{max}) [18] as shown in Table 2, which indicated that the experimental conditions were optimized and close to the theoretical limit in every concentration [19]. From above results, we find that ^{1}H NMR enhancement is positive correlation to MW power (P), concentration of ND and Raman peak intensity ratio of sp^2/sp^3; on the contrary, E_{exp} is approximate negative correlation to ND size (r).

Theoretically, ODNP enhancement E can be described as Eq. 1:

$$E = 1 - \xi s f |\gamma_S| / \gamma_I \quad (1)$$

where

$$s = \frac{\alpha P}{1 + \alpha P} = \frac{1}{1 + 1/(\alpha P)} \quad (2)$$

and

$$f = 1 - \frac{T_1}{T_{10}} = 1 - \frac{1/T_{10}}{1/T_1} \quad (3)$$

where ξ is the coupling factor, which is determined by the interaction between nucleus and electrons. s is the saturation factor (0~1) and related to MW power (P). α is a constant depending on the relaxation times of electron spins. f is the leakage factor (0~1), relating to the spin-lattice relaxation of the nucleus with (T_1) and without (T_{10}) unpaired electrons from surface defects of ND.

The T_1 and T_{10} in ND-water mixture may be different form the traditional organic small molecular radical (such as TEMPO), and can be compared to the relaxation distribution of water dispersion of paramagnetic protein solutions [20] or the effect of paramagnetic ions on solid surface on liquid relaxation [21] as Eqs. 4 and 5:

$$\frac{1}{T_{10}} = \frac{1}{T_{1B}} + R_s \times S = \frac{1}{T_{1B}} + R_s \times SSA \times C \quad (4)$$

$$\frac{1}{T_1} = \frac{1}{T_{10}} + R_e \times C_e = \frac{1}{T_{1B}} + R_s \times SSA \times C + R_e \times C_s \times (SSA \times C) \quad (5)$$

where T_{1B} is the bulk diamagnetic relaxation and R_s is the relaxivity constant arising from ideal ND surface without defect electrons. C is the ND concentration per unit volume in solution. S is the ND surface area per unit volume in solution. R_e is the relaxivity constant arising from unpaired electrons on surface. C_e is the unpaired electron concentration per unit volume in solution from ND surface defects. C_s is the surface defect concentration per unit area of the ND surface. SSA is the specific surface area of ND. For a practical ND sample, r is the average nanoparticle size of ND, SSA of practical ND sample can be expressed as (Eq. 6):

$$SSA = S_{RI} * 3/r \quad (6)$$

S_{RI} represents the effect of practical ND surface, including roughness, irregularity and nanoparticle-size uniformity [22,23]. Here, we define S_{RI} as "surface shape factor". If ND are ideal smooth and uniform spheres, the S_{RI} can be set as $S_{RI} = 1$. For a practical ND sample, the ODNP enhancement E can be re-expressed from formulas 1-6 as (Section 5 in Supporting information,):

$$E \approx 1 - \xi \frac{|\gamma_S|}{\gamma_I} \left(\frac{1}{1 + 1/(\alpha P)} \right) * \left(\frac{T_{1B} * R_e * C_s * C * \delta(sp^2/sp^3)}{r + T_{1B} * (R_s + R_e * C_s) * C * \delta(sp^2/sp^3)} \right) \quad (7)$$

here the coupling factor ξ is a positive value ($0 \leq \xi \leq 0.5$) [13]. As is known, the first order derivative of function $|E|$ can be used as the criterion of function changes. When $\xi s f |\gamma_S| / \gamma_I > 1$, the function $|E|$ is positive correlation to the parameters P, C, S_{RI} and $\delta(sp^2/sp^3)$; on the contrary, the function $|E|$ is negative correlation to the parameters r. The theoretical derivations are consistent with the above ODNP experimental results. The parameters C_s, r, SSA, and S_{RI} belong to characteristics of ND. Based on the theoretical derivations, a better ND polarizer has higher concentration of surface defect (C_s), smaller nanoparticle size (r), larger SSA, and higher S_{RI} by surface modification. However, surface modification *via* air oxidized reduced the weight of sp^2 hybridization and the concentration of surface defects (C_s) (Fig. S3 in Supporting information), resulting in no enhancement using air oxidized 30 nm ND (Fig. S4 in Supporting information). The surface defects were greatly reduced after air oxidized, which can be seen visually from ESR spectrum (Fig. S5 in Supporting information). Surface modification by oxidized provided a possibility for changing the surface properties of ND [24]. According to the above analysis, the larger the nanoparticle size is, the smaller the enhancement. As was expected, there was no enhancement for 1000 nm ND, due to the SSA of 1000 nm ND and the weight of sp^2 hybridization were much lower than small-size NDs, resulting in the very low concentration of surface defects (Fig. S6 in Supporting information).

Our study may provide a direction for further improving the performance of ND as polarizer and even as MRI contrast agent. Furthermore, the theoretical derivations may be also applicable for other nanomaterials polarizers. Therefore, when using ND polarizer, a higher enhancement can be realized by improving S_{RI} which will be beneficial for biological research at low concentration [25]. And the improved enhancement without changing particle size is conducive to further development the application under specific ND size [26]. Besides T_1 and T_2 are both influenced by ND size and concentration (Table 2), which is useful to contrast agent of MRI. Meanwhile, T_2 shows single-component distribution at all ND-water mixtures, further demonstrating the consistency of sample distribution and enhancement (Fig. S7 in Supporting information,).

In conclusion, we have achieved ^{1}H NMR enhancement to −22.5-fold *in-situ* liquid using ND polarizer at 0.06 T, proving the possibility of further improving the enhancement using ND as polarizer. We find that enhancement is related to following factors: Concentration of ND and Raman peak intensity ratio of sp^2/sp^3 are positive correlation to enhancement; on the contrary, ND size is negative correlation to enhancement. Furthermore, Raman spectra provides a good assistant method to evaluate the potential of ND for ODNP by crudely classifying ND based on sp^2/sp^3, which is beneficial to simplify the selection of NDs as polarizer. The greater enhancement of ^{1}H will further shorten experimental time and provide the possibility of *in-situ* tracking of ND.

Declaration of competing interest

The authors declare no competing financial interest.

Acknowledgments

We gratefully acknowledge Dr. Yugui He and Prof. Feng Deng for their assistance and insightful suggestions. This work was supported by the National key of R&D Program of China (No. 2018YFC0115000), the National Major Scientific Research Equipment Development Project of China (No. 81627901), the Chinese Academy of Sciences (Nos. YZ201677, YZ201551, KFJ-STS-QYZD-169), the National Natural Science Foundation of China (No. 11575287, 11705274), Major Scientific and Technological Innovation Project in Hubei (No. 2019AAA023), and Application Foundation Frontier Project of WuHan (No. 2019020701011450).

Supplementary materials

Supplementary material associated with this article can be found, in the online version, at doi:10.1016/j.cclet.2021.05.068.

References

[1] X.Q. Zhang, R. Lam, X. Xu, et al., Adv. Mater. 23 (2011) 4770–4775.
[2] N. Mohan, C.S. Chen, H.H. Hsieh, et al., Nano Lett. 10 (2010) 3692–3699.
[3] L.P. McGuinness, Y. Yan, A. Stacey, et al., Nat. Nanotechnol. 6 (2011) 358–363.
[4] N. Prabhakar, J.M. Rosenholm, Curr. Opin. Colloid. In. 39 (2019) 220–231.
[5] J.H. Du, L.M. Peng, Chin. Chem. Lett. 29 (2018) 747–751.
[6] W. Zhai, A. Lucini Paioni, X. Cai, et al., J. Phys. Chem. B 124 (2020) 9047–9060.
[7] G. Liu, M. Levien, N. Karschin, et al., Nat. Chem. 9 (2017) 676–680.
[8] A.W. Overhauser, Phys. Rev. 92 (1953) 411–415.
[9] P. Dutta, G.V. Martinez, R.J. Gillies, J. Phys. Chem. Lett. 5 (2014) 597–600.
[10] S. Kishimoto, M.C. Krishna, V.V. Khramtsov, et al., Antioxid. Redox Signal. 28 (2018) 1345–1364.
[11] K. Yasukawa, A. Hirago, K. Yamada, et al., Free Radic. Bio. Med. 136 (2019) 1–11.

[12] S. Matsumoto, H. Yasui, S. Batra, et al., Proc. Natl. Acad. Sci. U. S. A. 106 (2009) 17898–17903.
[13] D.E. Waddington, M. Sarracanie, H. Zhang, et al., Nat. Commun. 8 (2017) 1–8.
[14] J. Chen, J. Feng, F. Chen, et al., Fuel 257 (2019) 116107.
[15] E. Rej, T. Gaebel, D.E. Waddington, et al., J. Am. Chem. Soc. 139 (2017) 193–199.
[16] B.V. Yavkin, G.V. Mamin, M.R. Gafurov, et al., Magn. Reson. Solids 17 (2015) 15101.
[17] B. Yavkin, M. Gafurov, M. Volodin, et al., EPR and double resonances in study of diamonds and nanodiamonds, in: A.K. Shukla (Ed.), Experimental Methods in the Physical Sciences, Academic Press, Massachusetts, 2019, pp. 83–113.
[18] B.D. Armstrong, S. Han, J. Am. Chem. Soc. 131 (2009) 4641–4647.
[19] M. Bennati, C. Luchinat, G. Parigi, et al., Phys. Chem. Chem. Phys. 12 (2010) 5902–5910.
[20] G. Diakova, Y. Goddard, J.P. Korb, et al., J. Magn. Reson. 208 (2011) 195–203.
[21] I. Foley, S.A. Farooqui, R.L. Kleinberg, J. Magn. Reason. A 123 (1996) 95–104.
[22] M.W. Rotz, K.S. Culver, G. Parigi, et al., ACS Nano 9 (2015) 3385–3396.
[23] T. Peng, X. Zhang, Y. Huang, et al., Sci. Rep. 7 (2017) 46517.
[24] B.V. Yavkin, D.G. Zverev, G.V. Mamin, et al., J. Phys. Chem. C. 123 (2019) 22384–22389.
[25] V. Vaijayanthimala, P.Y. Cheng, S.H. Yeh, et al., Biomaterials 33 (2012) 7794–7802.
[26] J.I. Chao, E. Perevedentseva, P.H. Chung, et al., Biophys. J. 93 (2007) 2199–2208.